Multiscale modeling of PVDF matrix carbon fiber composites

2017 Modelling Simul. Mater. Sci. Eng. 25 045007

(http://iopscience.iop.org/0965-0393/25/4/045007)

IOP Publishing Modelling and Simulation in Materials Science and Engineering

Modelling Simul. Mater. Sci. Eng. **25** (2017) 045007 (15pp) https://doi.org/10.1088/1361-651X/aa6a8a

Multiscale modeling of PVDF matrix carbon fiber composites

Michael Greminger[1,3] **and Ghazaleh Haghiashtiani**[2]

[1] Department of Mechanical and Industrial Engineering, University of Minnesota Duluth, Duluth, MN 55812, United States of America
[2] Department of Mechanical Engineering, University of Minnesota, Minneapolis, MN 55455, United States of America

E-mail: mgreming@d.umn.edu and haghi004@umn.edu

Received 28 December 2016, revised 21 March 2017
Accepted for publication 31 March 2017
Published 19 April 2017

Abstract

Self-sensing carbon fiber reinforced composites have the potential to enable structural health monitoring that is inherent to the composite material rather than requiring external or embedded sensors. It has been demonstrated that a self-sensing carbon fiber reinforced polymer composite can be created by using the piezoelectric polymer polyvinylidene difluoride (PVDF) as the matrix material and using a Kevlar layer to separate two carbon fiber layers. In this configuration, the electrically conductive carbon fiber layers act as electrodes and the Kevlar layer acts as a dielectric to prevent the electrical shorting of the carbon fiber layers. This composite material has been characterized experimentally for its effective d_{33} and d_{31} piezoelectric coefficients. However, for design purposes, it is desirable to obtain a predictive model of the effective piezoelectric coefficients for the final smart composite material. Also, the inverse problem can be solved to determine the degree of polarization obtained in the PVDF material during polarization by comparing the effective d_{33} and d_{31} values obtained in experiment to those predicted by the finite element model. In this study, a multiscale micromechanics and coupled piezoelectric-mechanical finite element modeling approach is introduced to predict the mechanical and piezoelectric performance of a plain weave carbon fiber reinforced PVDF composite. The modeling results show good agreement with the experimental results for the mechanical and electrical properties of the composite. In addition, the degree of polarization of the PVDF component of the composite is predicted using this multiscale modeling approach and shows that there is opportunity to drastically improve the smart composite's performance by improving the polarization procedure.

[3] Author to whom any correspondence should be addressed.

Keywords: micromechanics, multiscale modeling, piezoelectric materials, smart composites, carbon fiber reinforced polymer, polyvinylidene difluoride (PVDF)

(Some figures may appear in colour only in the online journal)

1. Introduction

Smart composite materials are enabled by replacing the typical polymer matrix used in carbon fiber reinforced polymers with the piezoelectric polymer polyvinylidene difluoride (PVDF). When a stress is applied to these smart composites, the PVDF material generates a charge due to the piezoelectric effect. The resulting structure has strength and stiffness properties similar to conventional carbon fiber reinforced polymer structures, making it suitable for structural applications. Force sensing and structural health monitoring capabilities can be added to structures by replacing conventional carbon fiber composite materials with these smart composite materials. Traditionally, these sensing capabilities could only be included in a structure by attaching external strain gauges to the structure [1, 2]. The use of smart composites materials in structural applications that require structure health monitoring simplifies the implementation by not requiring the application of separate strain gauges and also allows strain to be measured in locations that were not previously possible such as between the layers of the composite laminate. In addition to structural health monitoring, piezoelectric smart composites can be used for energy harvesting to enable wireless sensing in applications that would be difficult to measure in any other way [3]. One area where wireless sensing is an enabling technology is for the structural health monitoring of wind turbine blades [4].

In previous work, the authors have experimentally characterized the piezoelectric and mechanical properties of the proposed smart composite material [5]. In this previous work, the piezoelectric coefficients were found to be lower for the smart composite than for the pure PVDF material. This is to be expected since the carbon fiber and Kevlar components carry a significant portion of the load, which impacts the amount of stress carried by the PVDF material. An open question in the previous work was whether the PVDF material was being fully polarized. In order to determine the degree of polarization, a modeling technique is required that predicts the piezoelectric properties of the composite structure based on the properties of the constituent materials. This article presents a method that can efficiently predict the electromechanical properties of the proposed smart composite structure. Note that, throughout this study, the piezoelectric coefficients are used as a proxy for the degree of polarization. Even though there is a direct relationship between remnant polarization and the piezoelectric coefficients, in general, this relationship is quite complex and is not usually known for a particular material and crystal structure [6].

Previous techniques for modeling piezoelectric composites have focused on the micromechanics approach of predicting the electromechanical properties of the composite at the scale of the inclusions [7–11]. These techniques have been shown to be accurate for predicting the properties at the microscale. However, a micromechanics approach alone is not sufficient for predicting the properties of the proposed smart composite structure. This is due to the millimeter scale properties of the composites. The millimeter scale properties come from the patterns of the plain weave carbon fiber and Kevlar fabrics in which the weft crosses over and under the warp. The mechanical properties of the weaves of textile composites have typically been modeled using a finite element approach [12, 13]. The second scale of the smart composite occurs at the scale of the carbon fiber and Kevlar tows that make up the

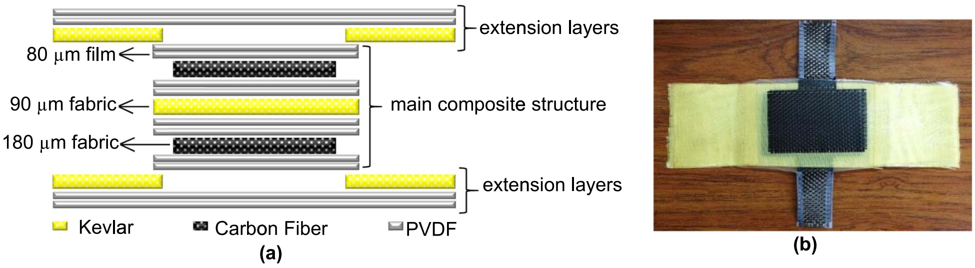

Figure 1. Structure of the proposed composite material. Cross sectional view of materials' stack-up and thicknesses before melt curing (a) and top view of final samples after melt curing (b). Reprinted from [14].

weaves. These tows are made up of micron scale continuous fibers. In order to predict the electrical and mechanical properties of the smart composite structure, a hybrid methodology is required that uses a micromechanics approach to predict the electromechanical properties of the Kevlar and carbon fiber tows and a coupled finite element approach to predict the electromechanical properties at the millimeter scale weave. This hybrid approach is introduced in this article. The contribution of this work is the use of a multiscale modeling approach to predict the performance of a piezoelectric matrix woven composite. Previous studies have only considered continuous fiber piezoelectric composites, which do not require a multiscale modeling approach. Also, this work is the first to consider a piezoelectric composite with two types of reinforcement fibers (both carbon fiber and Kevlar) in a sandwich structure, which is required in order to enable the sensing capabilities of the smart composite material.

The experimental characterization of the proposed smart composite structure is described in section 2. Section 3 describes the millimeter scale solid model and mesh of the composite weave structure. The micromechanics characterization of the Kevlar and carbon fiber tows is described in section 4. Section 5 summarizes the finite element modeling results of the smart composite structure and the conclusions are discussed in section 6.

2. Smart composite material properties and experimental characterization

In this section, the methods used for fabrication and polarization of the composite material are briefly explained. In addition, results from the experimental characterization of the mechanical and piezoelectric properties of the material are presented. More details on fabrication, polarization, and experimental characterization of the proposed composite structure can be found in the earlier work published by the authors [5].

2.1. Fabrication and polarization procedure

The reinforcement materials used for fabricating the proposed composite structure were two layers of carbon fiber and one layer of Kevlar fabric between them. Due to the electrical conductivity of carbon fiber material, these layers also acted as the electrodes for polarization and sensing purposes, which were separated from each other by the Kevlar dielectric layer. As shown in figure 1(a), two layers of PVDF film were placed between each of the reinforcement layers and on the top and bottom of the structure. Once melted, these PVDF layers formed the matrix of the composite structure. Since the characterization of the proposed smart composite

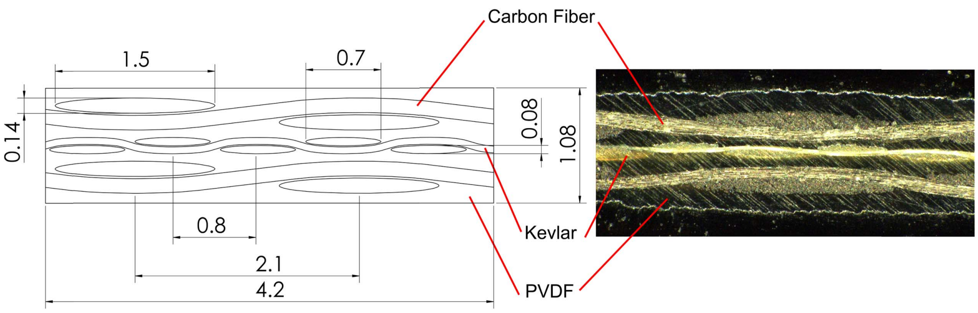

Figure 2. Dimensions in mm used for solid model on left and cross section of actual composite on right. Reprinted from [14].

involved tensile tests, extra layers of Kevlar and PVDF were added to the ends of the main structure of the composite to prevent the potential pressure introduced to the samples by the grips of the tensile test equipment (see figure 1(a)). The final samples (see figure 1(b)) were made by melt curing the stack of materials at 200 °C for 4 h under a pressure of 7 kPa.

The next step in preparing the smart composite structure was polarization to ensure the alignment of dipoles in the PVDF matrix. Due to the structure of the proposed composite, the common methods used for polarization of PVDF material were not feasible and special considerations were required. For instance, applying high electric fields would result in dielectric break down and stretching of the composite is not possible due to the high stiffness of carbon fiber and Kevlar layers. To overcome these limitations, a 2^3 full factorial design of experiment (DOE) was implemented to find the optimal condition of three factors (temperature, voltage, and duration of polarization) used in the polarization process. The experiments were performed at two levels of each of the factors. For each experiment, the effectiveness of polarization was evaluated in tensile tests as the ratio of the charge developed in the composite structure to the force applied to it. The analysis of the results showed that for the tested conditions, polarizing the samples by applying 2000 V at 75 °C for duration of 20 min would yield the highest degree of polarization and sample response.

2.2. Mechanical characterization

For the purpose of mechanical characterization, the Young's modulus of the composite structure was evaluated. A tensile load was applied to the composite material using MTS equipment and the resulting strain was recorded with an extensometer, which was attached to the samples. This test was replicated for different samples and with the extensometer attached at opposing sides to ensure that samples were not bending. Analyzing the obtained stress–strain plots yielded an average Young's modulus of 21.9 GPa for the proposed composite structure. It should be noted that the experimental elastic modulus given here differs from the value previously published [5] due to a change in the width dimension used in calculating the average stress. The width of the carbon fiber layers is used here rather than the entire width since the carbon fiber layers dominate the stiffness of the structure.

2.3. Piezoelectric characterization

The effective piezoelectric coefficients d_{31} and d_{33} were experimentally determined in tensile and compression tests, respectively. In each case, a cyclic load was applied to the samples and the charge developed in the smart composite material due to the applied load was extracted.

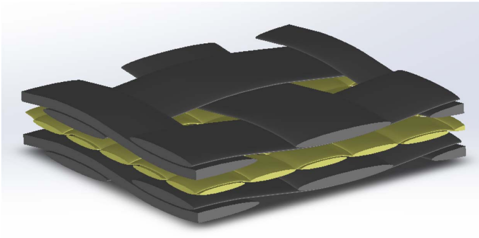

Figure 3. Solid model of carbon fiber and Kevlar weaves (PVDF matrix not shown). Reprinted from [14].

Table 1. Summary of the results obtained from experimental piezoelectric characterization of composite structure.

	Experimental d_{31}	Experimental d_{33}
Total force	15.90 N	176 N
Charge developed in the composite	0.480 pC	0.235 nC
Effective piezoelectric coefficient	0.000 44 pC N^{-1}	−1.95 pC N^{-1}

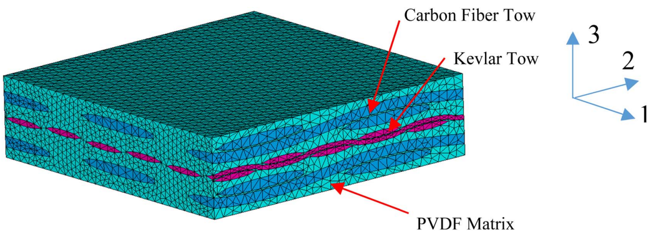

Figure 4. Finite element mesh of composite structure. The three direction is the direction of poling. Reprinted from [14].

The effective piezoelectric coefficient could then be calculated as:

$$(d_{3i})_{\text{eff}} = \frac{Q/A_{\text{CF,electrode}}}{\sigma_{\text{Average}_i}} \quad (\text{for } i = 1 \text{ or } 3), \tag{1}$$

where Q represents the charge developed in the composite structure due to the applied load, $A_{\text{CF,electrode}}$ is the area of carbon fiber electrode layer, and $\sigma_{\text{average}_i}$ is the average stress normal to either the 1-direction (along the structure's length) for d_{31} or the 3-direction (along the structure's thickness) for d_{33}. The results obtained from piezoelectric characterization of the proposed composite material are summarized in table 1. As it can be seen, the experimental characterization yielded the effective d_{31} and d_{33} coefficients of $4.36\,e^{-4}$pC N^{-1} and -1.95pC N^{-1}, respectively. These values differ from those previously published [5] since the average stress over the entire structure is used here, where, in the previous results, only the stress in the layer between the carbon fiber layers was used. This change was made to match the computation of the effective piezoelectric coefficients obtained from the finite element analysis discussed below. Also, the d_{33} value is assumed to be negative here to reflect the sign reported for PVDF d_{33} in the literature [15].

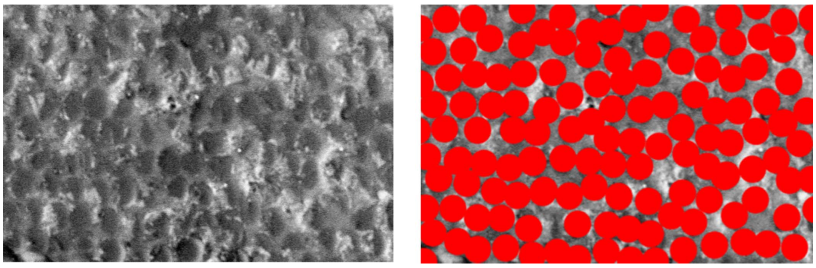

Figure 5. SEM image of carbon fiber tow cross section on left and manually placed dots representing fiber locations on right. The average carbon fiber diameter is 5.9 μm. Reprinted from [14].

3. Solid model and finite element mesh representation of the composite structure

Optical cross section images of the actual smart composite structures were used to determine the dimensions of the carbon fiber and Kevlar tows. These dimensions, along with a cross section image of the actual composite, are shown in figure 2. Using these dimensions, a solid model was constructed based on the smallest repeating pattern in the carbon fiber weave. This resulted in a solid model with a length and width of 4.2 mm and a height of 1.08 mm. The carbon fiber and Kevlar components of the solid model are shown in figure 3. Figure 4 shows the finite element mesh generated from this solid model. A tetrahedral mesh with mid-side nodes was used.

4. Micromechanics for the electromechanical properties of the carbon fiber and Kevlar tows

The smart composite structure is a multi-scale composite. The carbon fiber and Kevlar weaves, as shown in the previous section, are at the millimeter scale. However, the carbon fiber and Kevlar tows are composed of numerous micron scale fibers. Figure 5 shows a scanning electron microscope (SEM) image of a portion of one of the carbon fiber tows showing the numerous fibers surrounded by PVDF matrix that make up each of the tows.

One approach to model the properties for each of the tows would be to include the geometry of the individual carbon and Kevlar fibers in the finite element model. However, this would result in a finite element mesh with more elements than could be solved in a reasonable amount of time since the Kevlar fibers are 15 μm in diameter and the carbon fibers are 6 μm in diameter, both of which are three orders of magnitude smaller than the carbon fiber weave. For this reason, the electrical, mechanical, and piezoelectric properties will be computed numerically based on the electromechanical properties of the constituent materials. Both the micromechanics approach proposed by Dunn and Taya [7] and a finite element approach to computing the electromechanical properties of the tows will be explored in this section.

4.1. The dunn and taya micromechanics approach

An efficient method to numerically determine the effective elastic moduli for composite structures with high concentrations of inclusions was originally proposed by Tanaka and Mori and has become known as the Tanaka–Mori method [16]. Dunn and Taya extended this method to determine the combined dielectric, mechanical, and piezoelectric properties of piezoelectric composites [7]. The Dunn and Taya micromechanics approach is described below.

The orthotropic coupled piezoelectric and mechanical equations can be expressed as [8]:

$$\begin{bmatrix} \sigma_{11} \\ \sigma_{22} \\ \sigma_{33} \\ \sigma_{23} \\ \sigma_{13} \\ \sigma_{12} \\ D_1 \\ D_2 \\ D_3 \end{bmatrix} = \begin{bmatrix} C_{11} & C_{12} & C_{13} & 0 & 0 & 0 & 0 & 0 & e_{31} \\ C_{12} & C_{22} & C_{23} & 0 & 0 & 0 & 0 & 0 & e_{32} \\ C_{13} & C_{23} & C_{33} & 0 & 0 & 0 & 0 & 0 & e_{33} \\ 0 & 0 & 0 & C_{44} & 0 & 0 & 0 & e_{24} & 0 \\ 0 & 0 & 0 & 0 & C_{55} & 0 & e_{15} & 0 & 0 \\ 0 & 0 & 0 & 0 & 0 & C_{66} & 0 & 0 & 0 \\ 0 & 0 & 0 & 0 & e_{15} & 0 & \kappa_1 & 0 & 0 \\ 0 & 0 & 0 & e_{24} & 0 & 0 & 0 & \kappa_2 & 0 \\ e_{31} & e_{32} & e_{33} & 0 & 0 & 0 & 0 & 0 & \kappa_3 \end{bmatrix} \begin{bmatrix} \epsilon_{11} \\ \epsilon_{22} \\ \epsilon_{33} \\ 2\epsilon_{23} \\ 2\epsilon_{13} \\ 2\epsilon_{12} \\ E_1 \\ E_2 \\ E_3 \end{bmatrix}, \tag{2}$$

where C_{ij} are the components of the elastic stiffness matrix, e_{ij} are the piezoelectric coefficients in stress form, κ_i are the orthotropic dielectric permittivity constants, σ_{ij} are the stress components, D_i are the components of electric displacement, ϵ_{ij} are the components of strain, and E_i are the electric field components. The piezoelectric coefficients in stress form, e_{ij}, can be computed from the piezoelectric coefficients in strain form, d_{ij}, and the components of the elastic stiffness matrix, C_{ij}, using the following equation:

$$\begin{bmatrix} 0 & 0 & 0 & 0 & e_{15} & 0 \\ 0 & 0 & 0 & e_{24} & 0 & 0 \\ e_{31} & e_{32} & e_{33} & 0 & 0 & 0 \end{bmatrix} = \begin{bmatrix} 0 & 0 & 0 & 0 & d_{15} & 0 \\ 0 & 0 & 0 & d_{24} & 0 & 0 \\ d_{31} & d_{32} & d_{33} & 0 & 0 & 0 \end{bmatrix} \times \begin{bmatrix} C_{11} & C_{12} & C_{13} & 0 & 0 & 0 \\ C_{12} & C_{22} & C_{23} & 0 & 0 & 0 \\ C_{13} & C_{23} & C_{33} & 0 & 0 & 0 \\ 0 & 0 & 0 & C_{44} & 0 & 0 \\ 0 & 0 & 0 & 0 & C_{55} & 0 \\ 0 & 0 & 0 & 0 & 0 & C_{66} \end{bmatrix}. \tag{3}$$

Equation (2) can be rewritten as:

$$\boldsymbol{\Sigma} = \boldsymbol{E}\boldsymbol{Z}, \tag{4}$$

where $\boldsymbol{\Sigma}$ is the vector of stress and electric displacement values, $\boldsymbol{E}$ is the electromechanical material matrix, and $\boldsymbol{Z}$ represents the vector of strain and electric field values. Each constituent material in the continuous fiber composite will have its own material matrix $\boldsymbol{E}$. The combined electromechanical material matrix for the composite is obtained by combining the material matrices of the constituent materials in a weighted fashion using the following equation:

$$\boldsymbol{E}_{\text{composite}} = \boldsymbol{E}_{\text{matrix}} + c_{\text{fiber}}(\boldsymbol{E}_{\text{fiber}} - \boldsymbol{E}_{\text{matrix}})\mathbf{A}^{\boldsymbol{MT}}, \tag{5}$$

where c_{fiber} is the volume fraction of the inclusion phase of the composite and $\boldsymbol{A}^{\boldsymbol{MT}}$ is the Mori–Tanaka concentration matrix. Dunn and Taya [7, 17] provide a theoretical means to combine these material matrices where the concentration matrix can be obtained using the following set of equations:

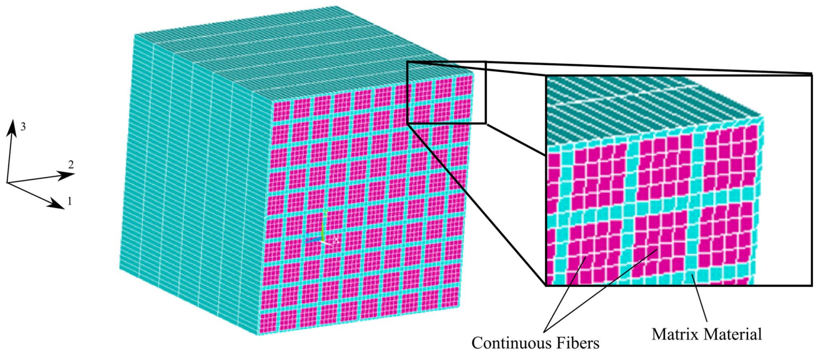

Figure 6. Unit cell used for finite element micromechanics study.

$$\boldsymbol{A}^{\mathrm{dil}} = [\boldsymbol{I} + \boldsymbol{S}\boldsymbol{E}_{\mathrm{matrix}}^{-1}(\boldsymbol{E}_{\mathrm{fiber}} - \boldsymbol{E}_{\mathrm{matrix}})]^{-1}, \tag{6}$$

$$\boldsymbol{A}^{\mathrm{MT}} = \boldsymbol{A}^{\mathrm{dil}}[c_{\mathrm{matrix}}\boldsymbol{I} + c_{\mathrm{fiber}}\boldsymbol{A}^{\mathrm{dil}}]^{-1}, \tag{7}$$

where $\boldsymbol{A}^{\mathrm{dil}}$ is the dilute approximation of the concentration matrix, $\boldsymbol{I}$ is the identity matrix, and $\boldsymbol{S}$ is the matrix representation of the Eshelby's constraint tensor for an ellipsoid occlusion. The constraint matrix $\boldsymbol{S}$ has been extended by Dunn and Taya to consider the coupled electromechanical behavior required for piezoelectric composite materials. The constraint tensor can be expressed as the following integrals over the unit sphere [17]:

$$S_{MnAb} = \begin{cases} \dfrac{a_1a_2a_3}{8\pi}\displaystyle\int_{|z|=1}\frac{1}{\zeta^3}[G_{mJin}(z) + G_{nJim}(z)]\mathrm{d}S(z), & M = 1, 2, 3, \\ \dfrac{a_1a_2a_3}{4\pi}\displaystyle\int_{|z|=1}\frac{1}{\zeta^3}G_{4Jin}(z)\mathrm{d}S(z), & M = 4, \end{cases} \tag{8}$$

where $|z| = 1$ is the surface of the unit sphere, and:

$$\zeta = [a_1^2z_1^2 + a_2^2z_2^2 + a_3^2z_3^2]^{\frac{1}{2}}, \tag{9}$$

where a_1, a_2, and a_3 are the lengths of the semi-axes of the ellipsoidal inclusion, and:

$$G_{MJin}(z) = z_iz_nK_{MJ}^{-1}(z), \tag{10}$$

where:

$$K_{MJ} = E_{iJMn}z_iz_n. \tag{11}$$

Equations (8), (10) and (11) make use of standard indicial notation, where repeated indices indicate summation, with the addition that lower case indices take on the values 1–3 and upper case indices take on the values 1–4. Note that the constraint tensor S_{MnAb} can be evaluated for a continuous fiber inclusion by taking the limit as one of a_1, a_2, or a_3 tend to infinity. For the continuous fiber composite materials evaluated here, the 1-direction is taken as the fiber direction, so the integrals in (8) are evaluated for the case when a_1 tends towards infinity. In addition, for the case of continuous fiber inclusions, the integrals in (8) cannot be evaluated analytically. The python function *quad* from the library *mpmath* was used to numerically evaluate these integrals [18].

4.2. The finite element micromechanics approach

In order to validate the Dunn and Taya method for the continuous fiber smart composite materials used in this work, the results of computing the tow properties using (5)–(11) were

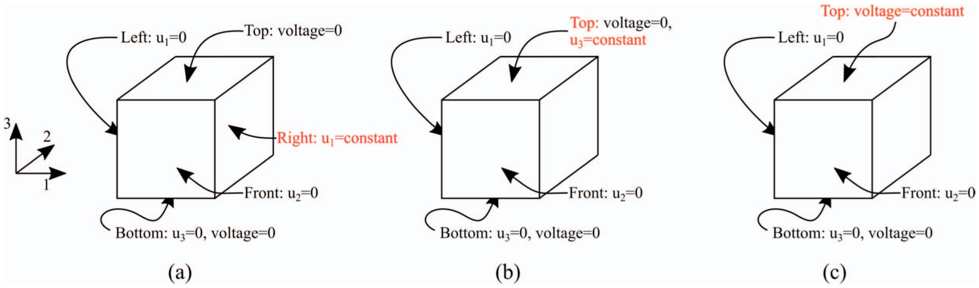

Figure 7. Boundary conditions used for finite element analysis. Boundary conditions for the determineng E_{11} and d_{31} (a), boundary conditions for determining E_{33} and d_{33} (b), and boundary conditions for determining κ_{33} (c).

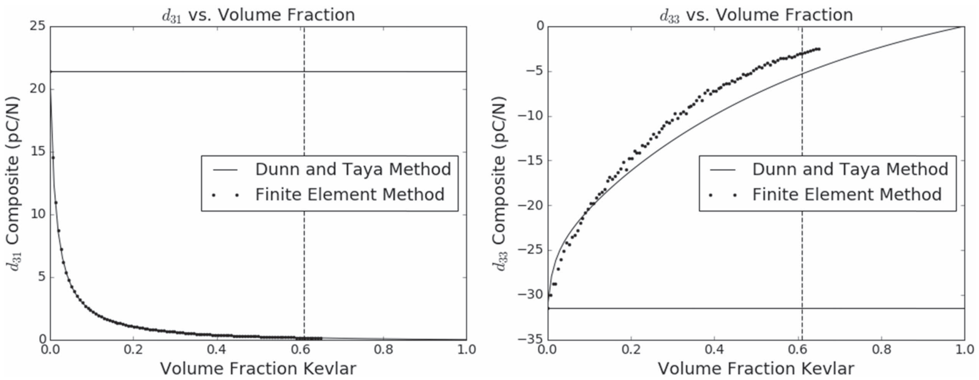

Figure 8. Piezoelectric coefficients versus Kevlar volume fraction.

compared to the results obtained using finite element analysis. Figure 6 shows the unit cell that was used for the finite element micromechanics study. The unit cell has been divided into the matrix material and the fiber material. Square geometry was used for the fibers to facilitate a quadrilateral mesh to provide accuracy with fewer elements. A total of 100 fibers were included in the unit cell model with all of the fibers together making up 65% of the volume of the unit cell. Volume fractions between 0% and 65% were modeled by randomly assigning some of the fiber elements to the matrix material. Using this technique, volume fractions between 0% and 65% could be modeled using a single finite element mesh. The main limitation to this approach for computing the micromechanical properties is that high volume fractions cannot be computed since the element quality degrades leading to artificial stiffening in the direction transverse to the fibers. Because of this, the maximum volume fraction was limited to 65% for this micromechanics approach. This is an acceptable constraint since the volume fraction of the actual composites is below this 65% point. ANSYS was used to perform the modeling using the SOLID226 electrical-mechanical coupled field element type (20-node quadrilateral element). The *Electroelastic and Piezoelectric* coupled-field analysis type was chosen for the elements, which couples the electrostatic, elastic, and piezoelectric physics of the material. The elastic moduli, piezoelectric coefficients, and relative permittivity of the unit cell were modeled. The boundary conditions used for the finite element analysis are shown in figure 7.

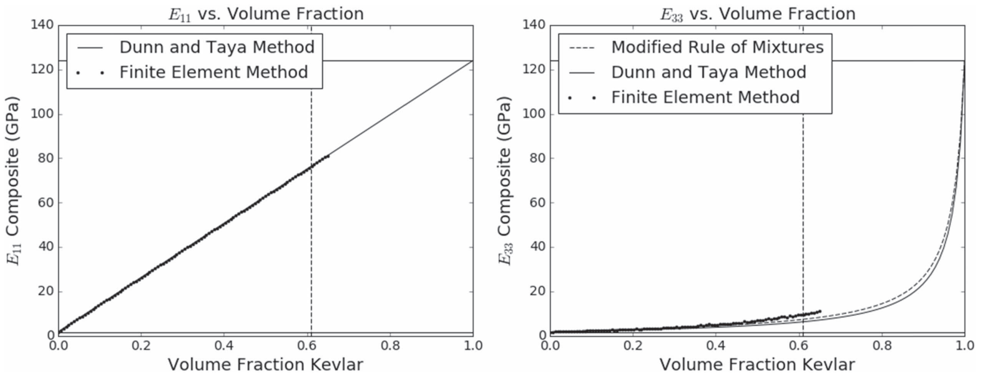

Figure 9. Elastic moduli versus Kevlar volume fraction.

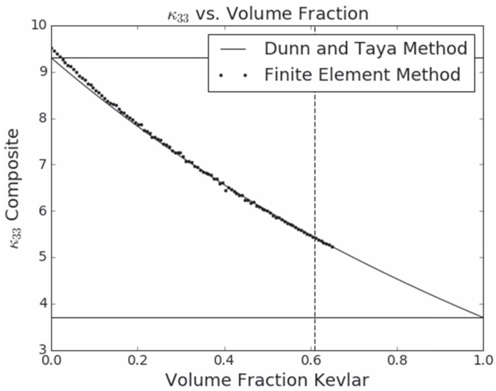

Figure 10. Relative permittivity versus Kevlar volume fraction.

4.3. Micromechanics results

The results of applying the Dunn and Taya method and the finite element approach to the Kevlar tows are shown in figures 8–10. For the Kevlar tows, the 1-direction is aligned with the fibers and the poling direction is the 3-direction. In addition to the results from Dunn and Taya method and the finite element approach, the modified rule of mixtures calculation of the transverse modulus E_{33} is included [19]. The properties used for the constituent materials are summarized in table 2.

The E_{11} direction elastic modulus (the along fiber direction) values are indistinguishable between the two methods. For the cross-fiber direction elastic modulus, E_{33}, the finite element analysis gives a slightly higher stiffness. This higher stiffness in the transverse direction leads the finite element model to predict a lower d_{33} piezoelectric coefficient as compared to the Dunn and Taya method. The d_{31} piezoelectric coefficients and the relative permittivity values determined by each method are nearly indistinguishable. The higher transverse elastic modulus from the finite element method compared to the Tanaki–Mori method is consistent with other results in the literature when a square arrangement of fibers is used [23]. The Dunn and Taya method and the finite element approach were only compared for the Kevlar tows, however, similar agreement between the two methods is expected for the carbon fiber tows.

Table 2. Material properties used for constituent materials.

Material	Elastic modulus (GPa)	Poisson's ratio	Relative permittivity	d_{31} (pC N^{-1})	d_{32} (pC N^{-1})	d_{33} (pC N^{-1})
PVDF	1.72 [20]	0.35 [21]	9.3 [20]	21.4 [15]	2.3 [15]	−31.5 [15]
Kevlar 49	124 [19]	0.45 [19]	3.7 [22]	—	—	—
Carbon fiber (33 MSI)	228 [19]	0.25 [19]	—	—	—	—

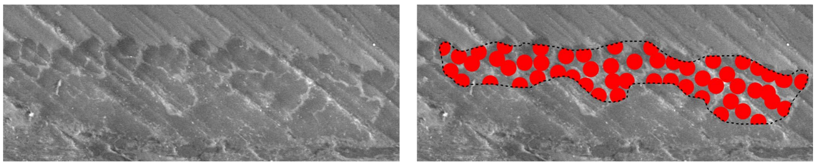

Figure 11. SEM image of Kevlar fiber tow cross section on the left and manually placed dots representing fiber locations on the right. The area used for the volume fraction calculation is indicated by a dashed line. The average Kevlar fiber diameter is 14.6 μm.

Given the good agreement between the Dunn and Taya method and the finite element approach for computing the composite tow electromechanical properties, the Dunn and Taya method will be used to compute both the Kevlar and carbon fiber tow properties for the results presented in section 5.

4.4. Determination of kevlar and carbon fiber volume fractions

The weighting of the electromechanical material matrices depends on the volume fraction of fibers in the composite. The volume fraction for both the carbon fiber and Kevlar tows were computed from SEM images. Figure 5 shows one image that was used to compute the volume fraction of carbon fibers and figure 11 shows one image that was used to compute the volume fraction of Kevlar fibers. Several SEM images were used in computing the carbon fiber and Kevlar volume fractions yielding an average carbon fiber volume fraction of 55% and an average Kevlar volume fraction of 61%. The dashed vertical line in figures 8–10 represent the measured Kevlar volume fraction of 61%.

With the volume fractions computed, the composite electromechanical material matrix can be calculated for the carbon fiber and Kevlar tows in order to model the full smart composite weave structure. The values of the parameters for the constituent materials used in computing the tow properties are summarized in table 2. Since the goal of this study is to determine the degree of poling achieved in the PVDF component of the composite, multiple values for the PVDF piezoelectric coefficients were modeled, as will be discussed in the following section.

5. Finite element analysis of the smart composite weave

Using the full orthotropic electromechanical material matrices for the carbon fiber and Kevlar tows obtained from the Dunn and Taya method, the smart composite material was modeled based on the finite element mesh shown in figure 4. The mesh is a representative volume of the smart composite and was sized to contain the smallest repeating pattern of the reinforcement weave, which resulted in a model size with a length and width of 4.2 mm. The mesh represents the entire 1.1 mm thickness of the smart composite and contains both the carbon fiber and Kevlar layers. ANSYS was used to perform the modeling with the SOLID227 electrical-mechanical coupled field element type (10-node tetrahedral element). Similar to the micromechanics finite element analysis above, the *Electroelastic and Piezolectric* coupled-field analysis type was used for these elements. The elastic moduli and piezoelectric coefficients were obtained using the boundary conditions shown in figure 7. In addition, the capacitance of the composite structure was modeled. The coordinate system is shown in figure 4 where the 3-direction is the poling direction of the composite structure.

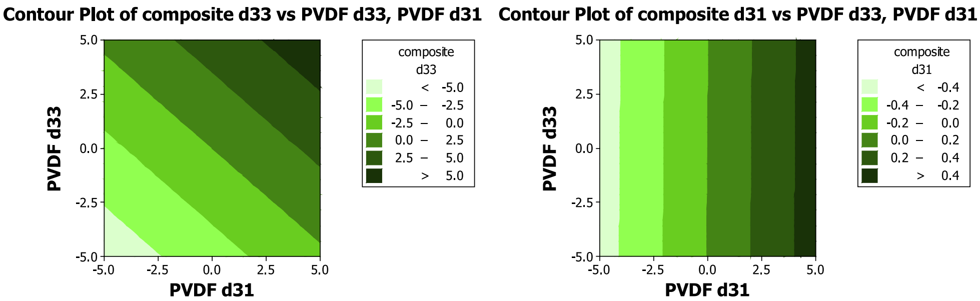

Figure 12. Countour plots for the response surface relating the PVDF piezoelectric coefficients to the composite piezoelectric coefficients.

Table 3. Comparison of finite element and experimental smart composite properties.

Source	d_{31} (pC N^{-1})	d_{33} (pC N^{-1})	E_{11} (GPa)	Capacitance (pF)
Experiment	0.000 44	−1.95	21.9	585
Finite element model	−0.000 62	−1.95	21.7	492

Since the main aim of the finite element modeling was to determine the degree of polarization obtained in the PVDF component of the composite, a 3^2 factorial modeling DOE was performed where all possible combinations of three levels of PVDF d_{31} and d_{33} were modeled. A quadratic response surface was fit to the DOE results to determine the values of the PVDF piezoelectric coefficients required for obtaining the corresponding experimental effective coefficients. Figure 12 shows the response surface that was fit to the DOE results. Using this technique, it was determined that a d_{31} of -0.015 pC N^{-1} and a d_{33} of -2.7 pC V^{-1} were required from the PVDF to obtain the experimental effective piezoelectric coefficients of the smart composite structure. Table 3 summarizes the finite element modeling results using these PVDF piezoelectric coefficients, and compares those results to the experimental measurements of the composite structure.

6. Conclusions

In this work, a multiscale micromechanics methodology was combined with finite element modeling to predict the mechanical and piezoelectric performance of a plain weave carbon fiber reinforced PVDF composite. As seen in table 3, there is good agreement between the modeled and experimental piezoelectric d_{33} values since the PVDF piezoelectric coefficients in the model were chosen to match the experimental values. However, the d_{31} value did not match as well as the d_{33} value. This is due to the effective d_{31} value of the composite being so low that it is below the error threshold of the response surface fit to the modeling DOE results. This low d_{31} value will be addressed below. There is also good agreement with the elastic modulus and capacitance values using the published mechanical and dielectric properties of the constituent materials. The good agreement for the elastic modulus and the capacitance between the experimental and modeled data validates using this model to predict the piezoelectric coefficients of the PVDF phase of the composite.

Through finite element modeling of the smart composite structure, it was found that the polarization process obtains a PVDF component d_{31} value of $-0.015\,\mathrm{pC\,N^{-1}}$ and a d_{33} value of $-2.7\,\mathrm{pC\,N^{-1}}$. The d_{31} value obtained is about three orders of magnitude smaller than would be expected for a fully polarized PVDF material and the d_{33} value is about one order of magnitude smaller than would be expected for a fully polarized PVDF material (see table 2 for typical d_{31} and d_{33} values for a fully polarized PVDF material). This indicates that there is opportunity to increase the sensitivity of the proposed smart composite structure by at least an order of magnitude by improving the polarization process. Also, the disproportionally low d_{31} value indicates that the crystal structure of the PVDF phase may not match the crystal structure normally obtained in polarized PVDF structures. An investigation of the crystalline structure will be pursued in future work to characterize the polarization of the PVDF in a similar fashion to what has been done in other studies [24].

Acknowledgments

This work was supported in part by the Swenson College of Science and Engineering at the University of Minnesota Duluth and by Grant-in-Aid funding from the University of Minnesota.

References

[1] Staszewski W, Boller C and Tomlinson G R 2004 *Health Monitoring of Aerospace Structures: Smart Sensor Technologies and Signal Processing* (New York: Wiley)
[2] Giurgiutiu V and Soutis C 2012 Enhanced composites integrity through structural health monitoring *Appl. Compos. Mater.* **19** 813–29
[3] Lynch J P and Loh K J 2006 A summary review of wireless sensors and sensor networks for structural health monitoring *Shock Vib. Dig.* **38** 91–130
[4] Swartz R A, Lynch J P, Zerbst S, Sweetman B and Rolfes R 2010 Structural monitoring of wind turbines using wireless sensor networks *Smart Struct. Syst.* **6** 183–96
[5] Haghiashtiani G and Greminger M A 2015 Fabrication, polarization, and characterization of PVDF matrix composites for integrated structural load sensing *Smart Mater. Struct.* **24** 045038
[6] Turik A V, Topolov V Y and Aleshin V I 2000 On a correlation between remanent polarization and piezoelectric coefficients of perovskite-type ferroelectric ceramics *J. Phys. D: Appl. Phys.* **33** 738
[7] Dunn M L and Taya M 1993 An analysis of piezoelectric composite materials containing ellipsoidal inhomogeneities *Proc.: Math. Phys. Sci.* **443** 265–87
[8] Odegard G M 2004 Constitutive modeling of piezoelectric polymer composites *Acta Mater.* **52** 5315–30
[9] Chan H L W and Unsworth J 1989 Simple model for piezoelectric ceramic/polymer 1–3 composites used in ultrasonic transducer applications *IEEE Trans. Ultrason. Ferroelectr. Freq. Control* **36** 434–41
[10] Lin C-H and Muliana A 2013 Micromechanics models for the effective nonlinear electro-mechanical responses of piezoelectric composites *Acta Mech.* **224** 1471–92
[11] Ho C H, Poon Y M and Shin F G 2006 New explicit formulas for the effective piezoelectric coefficients of binary 0–3 composites *J. Electroceramics* **16** 283–8
[12] Tan P, Tong L and Steven G P 1997 Modelling for predicting the mechanical properties of textile composites—a review *Composites* A **28** 903–22
[13] Barbero E J, Trovillion J, Mayugo J A and Sikkil K K 2006 Finite element modeling of plain weave fabrics from photomicrograph measurements *Compos. Struct.* **73** 41–52
[14] Greminger M and Haghiashtiani G 2015 Finite element modeling of PVDF matrix carbon fiber composites *Int. Workshop on Structural Health Monitoring (IWSHM 2015) (Stanford, California)*

[15] Nalwa H S 1995 *Ferroelectric Polymers: Chemistry: Physics, and Applications* (Boca Raton, FL: CRC Press)
[16] Mori T and Tanaka K 1973 Average stress in matrix and average elastic energy of materials with misfitting inclusions *Acta Metall.* **21** 571–4
[17] Dunn M L and Taya M 1993 Micromechanics predictions of the effective electroelastic moduli of piezoelectric composites *Int. J. Solids Struct.* **30** 161–75
[18] Johansson F *et al* 2014 mpmath: a python library for arbitrary-precision floating-point arithmetic (version 0.19)http://mpmath.org/
[19] Laszlo G S S and Kollar P 2009 *Mechanics of Composite Structures* (Cambridge: Cambridge University Pres)
[20] 'Professional Plastics, PVDF Film—Material Data Sheet': http://professionalplastics.com/professionalplastics/content/PVDFFilmDataSheet.doc (Accessed: 31-May-2015)
[21] Furukawa T, Wen J X, Suzuki K, Takashina Y and Date M 1984 Piezoelectricity and pyroelectricity in vinylidene fluoride/trifluoroethylene copolymers *J. Appl. Phys.* **56** 829–34
[22] Minges M L 1989 *Electronic Materials Handbook: Packaging* vol 1 (Materials Park, OH: ASM International)
[23] Benedikt B, Rupnowski P and Kumosa M 2003 Visco-elastic stress distributions and elastic properties in unidirectional composites with large volume fractions of fibers *Acta Mater.* **51** 3483–93
[24] Riosbaas M T, Loh K J, O'Bryan G and Loyola B R 2014 *In situ* phase change characterization of PVDF thin films using raman spectroscopy *SPIE Smart Structures and Materials + Nondestructive Evaluation and Health Monitoring* p 90610Z